Chemical Physics Letters 687 (2017) 38–43

Contents lists available at ScienceDirect

Chemical Physics Letters

journal homepage: www.elsevier.com/locate/cplett

Research paper

An X-ray and computational study of liquid pentylammonium nitrate

Lorenzo Gontrani [a,*], Francesca Leonelli [a], Marco Campetella [a,b,*]

[a] Università degli Studi di Roma "La Sapienza", P. le Aldo Moro 5, I-00185 Roma, Italy
[b] Chimie ParisTech, PSL Research University, CNRS, Institut de Recherche de Chimie Paris, F-75005 Paris, France

ARTICLE INFO

Article history:
Received 22 May 2017
In final form 30 August 2017
Available online 1 September 2017

Keywords:
X-ray
Nitrate
Pentylammonium
Vibrations
Ionic liquids

ABSTRACT

In this article we report the study of liquid pentylammonium nitrate with Wide Angle X-ray scattering and AIMD simulations. Static and dynamical features were characterized by comparing the experimental X-ray pattern with *ab initio* molecular dynamics simulation trajectories. From the analysis, we were able to focus our attention on the nature and time duration of the hydrogen bond network established between cation and anion. Such H-bond interactions occur around 2.8 Å, last about 1.55 ps and lead to the loss of degeneracy of the asymmetric stretching normal mode of the anion, with a splitting of about 84 cm^{-1}.

1. Introduction

Ionic liquids (ILs) are salts with a melting point below 100 °C, and they are composed of a cation and an anion. The discovery of ionic liquids is generally attributed to Paul Walden [1], who described a series of water-free salts with a melting point below 100 °C. Among the compounds described by Walden was included the widely known ethylammonium nitrate (EAN), melting point 12–14 °C, that is commonly defined as RTIL ("Room Temperature Ionic Liquid") in the modern sense. About six decades after Walden's paper, the interest and the scientific literature about these compounds flourished, owing to their peculiar properties, that have been described extensively in several papers, to which the reader is referred for brevity [2–6]. EAN is one member of the family of alkylammonium nitrates that belongs to the subgroup of protic ionic liquids (PILs), and can be obtained from the proton transfer reaction between the *Brønsted acid* nitric acid and the *Brønsted base* alkylamine.

The reaction leads to the formation of a neat liquid made up of ion pairs where proton acceptor and donor sites eventually generate a hydrogen-bond network [7–9]. In this paper, we deal with pentylammonium nitrate (PeAN, $C_5H_{14}NH_3^+ \cdot NO_3^-$) (see Fig. (1)), a low-melting point solid just beyond the upper-temperature border of the liquid window of alkylammonium nitrates (ethyl, propyl and butylammonium (EAN, PAN, BAN)); indeed, its melting temperature was found to be 45 ± 1 °C, when it becomes a colorless dense liquid, and remains undercooled down to below 30 °C.

The literature mentioning this compound is very scarce, and limited (to our knowledge) to a couple of studies by Greaves et al., that reported its Small and Wide Angle X-ray Scattering pattern (S-WAXS) collected at 50 °C [10] and 60 °C [11] within two systematic surveys on PILs. They found three main peaks at Q = 0.39, 1.55/1.51 and 2.53 $Å^{-1}$, that correspond to effective correlation distances ($2\pi/q$) of 15.94, 4.05/4.15 and 2.48 Å, respectively.

In all PILs, the main interaction responsible for the condensed phase aggregation is the strong hydrogen bond between cation ammonium group and anion oxygen. Regarding the anion, it is known [12] that the molecule *in vacuo* belongs to D_{3h} symmetry group, and has a total of six normal modes: ν_1, totally symmetric stretching, ν_3 asymmetric stretching, ν_4 in-plane deformation, ν_2, out-of-plane deformation; ν_3 and ν_4 are doubly degenerate. Recent works [13,14] have shown that nitrate anion in condensed phase, owing to the interaction with the environment, lowers its symmetry from D_{3h} to C_{2v} group. Such symmetry breaking leads to a splitting of the asymmetric stretching band. Furthermore, in PILs the hydrogen bond interactions lead to the N—H stretching band broadening [15] and increase the disorder of the phase [16,15]. For instance, because of polarization effects, the anions of methylammonium nitrate (MAN) exhibit a not complete or saturated hydrogen bond network [17,18].

Therefore, the role of such effects hinders a realistic simulation of PeAN static and dynamical properties with classical molecular dynamics (MD), where they are neglected. For example, the calculation of hydrogen bond radial distribution functions (RDFs) and lifetimes [19] requires to go beyond the classical MD scheme and

* Corresponding authors.
E-mail addresses: lorenzo.gontrani@uniroma1.it (L. Gontrani), marco.campetella@uniroma1.it (M. Campetella).

http://dx.doi.org/10.1016/j.cplett.2017.08.068
0009-2614/

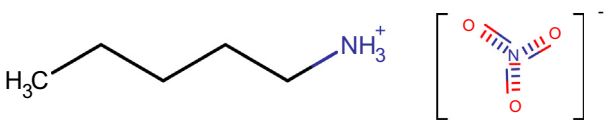

Fig. 1. Sketch of cation and anion: pentylammonium (left) and nitrate (right).

to use a more refined computational approach [20,21]. We present in this work, for the first time, the experimental X-ray diffraction patterns of bulk liquid PeAN in the spatial range of the short-medium distances, i. e. from 0 to 24 Å approximately. In order to interpret the experimental data we exploit *ab initio* molecular dynamics (AIMD), from which trajectory we also calculated some parameters of the hydrogen bonding network, namely the radial distribution functions (RDFs) - static parameter - and the normal mode analysis of the anions - dynamical. Finally we evaluated the cation–anion potential of mean force using Umbrella Sampling.

2. Experimental details

Solvents (LC-MS grade), pentylamine was purchased from Aldrich, Nitric acid (65% w/w) from Carlo Erba. ^{1}H and ^{13}C NMR spectra were recorded on a Varian Mercury 300 at 300.13 and 75.48 MHz, respectively; δ in ppm relative to the residual solvent peak of DMSO-d6 at 2.50 and 39.5 ppm for ^{1}H and ^{13}C, respectively. To a solution of pentylamine (10 mL, 86 mmol) in pentane (10 mL), cooled at −20 °C, HNO_3 (65% wt/wt, 6.1 mL, 86 mmol) was cautiously added dropwise while stirring. The reaction mixture was stirred for 2 h at the same temperature and after that time the pentane layer was separated, the product washed with pentane and dried at the rotary evaporator. The residual water was removed, while stirring, on standing under high vacuum pump for 72 h and the water final quantity was evaluated by ^{1}H NMR analysis (H_2O < 0.003 wt.%). The compound was kept under a nitrogen atmosphere. Data of PeAN: white solid; ^{1}H NMR (DMSO-d6): 7.79 (s, 3H), 2.77 (t, J = 7.5, 2H), 1.51 (pquint, J = 7.5, 2H), 1.35–1.15 (m, 4H), 0.84 (t, J = 6.7, 3H); ^{13}C NMR (DMSO-d6): 39.0, 28.0, 26.8, 21.8, 13.8. The X-ray experiments were performed on a new Energy-Dispersive diffractometer recently set up in our lab at Rome "La Sapienza" university. The instrument has a novel horizontal design and uses the Bremsstrahlung radiation of a X-ray tube with tungsten target [22–25]. Data acquisition is carried out at three to four fixed angular configurations in parallel, very rapidly and at large momentum transfer range Q, namely between 0.15 and 24 Å^{-1}. The magnitude of Q depends on the scattering angle according to the relation $Q = 4\pi sin(\theta)/\lambda$, approximately equal to ≈1.0136 E sin θ, if E is expressed in keV and Q in Å^{-1}. The marked increase of diffracted intensity achievable in this new instrumental configuration allows to collect a complete diffraction pattern at high statistics (*viz* more than 500,000 counts for every experimental point at each scattering angle), in at most 6 h (see Fig. 2).

Fig. 2. EDXD_3H, the new EDXD diffractometer with three simultaneous detectors.

Furthermore, the open configuration of the instrument allows the easy use of additional equipment, such as the spot fan heater used to melt and keep the sample liquid. The sample was put in a quartz capillary, and the beam was focussed on the liquid portion at the center of the capillary, surrounded by solid phases above and below. In the data treatment procedure, the diffracted intensity is normalized to white beam radiation, to sample/capillary adsorption and to the scattering of an isolated electron ("electron units"), and finally the independent atomic scattering and the Compton incoherent scattering contributions are subtracted [23], to yield the structure function or "reduced intensity" I(Q):

$$I(Q) = I_{EXP}(Q)_{E.U.} - \sum_{i=1}^{N} x_i f_i^2 - I_{Incoh} \quad (1)$$

The structure function depends on the pairwise distances between the atoms of the system:

$$I(Q) = \sum_{i=1}^{N}\sum_{j=1}^{N} x_i x_j f_i f_j \times \left[4\pi\rho_0 \int_0^{\infty} r^2 (g_{ij}(r) - 1)\frac{sinQr}{Qr} dr\right] \quad (2)$$

Eq. (2) is the link between experimental and model data, as the g(r)'s can be calculated from molecular simulations.

The radial distribution profile, in differential form, was obtained by I(Q) Fourier Transform:

$$Diff(r) = \frac{2r}{\pi}\int_0^{\infty} QI(Q)M(Q)rsinQdQ \quad (3)$$

In the formulae above, x_i are the numerical concentrations of the species, f_i their Q-dependent coherent X-ray scattering factors and ρ_0 is the bulk number density of the system. To improve the curve resolution at high Q, and to decrease the truncation errors, both the experimental and the theoretical structure functions were multiplied by a sharpening function $M(Q) = \frac{f_N^2(0)}{f_N^2(Q)} exp^{-0.01Q^2}$ (see [8,24] and references cited therein for more details; a thorough discussion on the calculation of X-ray scattering signals can be found in [26]).

3. Computational details

The simulation cell of PeAN bulk liquid contained 32 IL pairs. In the first pre-equilibration phase, a classical equilibration dynamics of about 5 ns in the NPT *ensemble* was performed, using the AMBER [27] program with Gaff [28] force field. The box edge (L) and the relative density were respectively 20.2 Å and 1.02 g/cm^3, differing by only 0.8% from the measured value (1.0118). The final configuration of the trajectory was used as the starting point for the *ab initio* simulations, that were performed with CP2k [29], using the Quickstep module [30] and the orbital transformation [31]. PBE density functional [32] was used for the electronic calculation, with the empirical dispersion correction (D3) by Grimme [33]. MOLOPT-DZVP-SR-GTH basis sets [34] and GTH pseudopotentials [35] were applied; a 0.5 fs time step was employed, and the simulation temperature was set at 310 K by a Nosé-Hoover chain thermostat [36]. Firstly, an equilibration of 7 ps was run, followed by a production NVT dynamics of 40 ps. To compute the free energy plot of the pair interaction, we exploited the Umbrella Sampling (US) technique [37] on a smaller box composed of ten ion pairs. The N(Cat)···O(Ani) distance was chosen as biased collective variable. A total of 36 constrained simulations, lasting 20 ps each, was implemented. The MOLSIM package [38] was used to perform the anion vibrational analysis. In this way the effective normal modes were obtained directly from the velocity density of states (VDOS),

calculated from the fourier transform (FT) of the velocity autocorrelation function. For more details refer to [14].

4. Results

In Fig. 3 the structure factor [QI(Q)M(Q), top] and radial distribution function [Diff(r), bottom] are reported. The experimental data are in black, the theoretical ones in red; the 0–4 $Å^{-1}$ range is plotted in the inset.

The presence of the following characteristic features can be found in the experimental I(Q): (1) pre-peak at 0.37 $Å^{-1}$, (2) principal peak at 1.60 $Å^{-1}$, and (3) two smaller peaks (2.65 and 4.12 $Å^{-1}$). These findings comply with the peaks reported by Greaves et al. [10,11] also considering that our measure was conducted at lower temperature. As already discussed in the literature, the presence of a medium-range order in the liquids gives rise to a peak in the structure factor curve, located at Q values less then 1 Å [7,39]. Though the sensitivity of EDXD instrument at very low Q values is smaller than that of a dedicated SAXS diffractometer, the pre-peak feature is clearly visible. The data also correlate satisfactorily with a powder-diffraction measurement on solid PeAN (see Fig. 4), that show the three peaks at 0.384, 1.544 and 2.516. Anyhow, we decided to limit our model to the pair correlations present at distances up to 10 Å; the system size and the most accurate simulation method for that size was chosen accordingly.

Overall, good reproduction of the experimental data, both QI(Q)M(Q) and Diff(r), by our theoretical model can be achieved. By looking in detail, the pre-peak produces a far-ranging shell structure (the correlation extends up to about 14 Å), whereas the theoretical function abruptly stops at about 10 Å due to the limited length of the box. The principal peak contains all the intermolecular contacts that correspond to the first and second shell structure of the liquid, while the third feature is related to the intermolecular cation–anion hydrogen-bond interactions [40]. The main disagreement regards the excessively deep trough around 6.5 Å, that is related to the fake shoulder around 0.8 $Å^{-1}$, probably due to an over-estimation of charge-charge correlations [41]. After endorsing

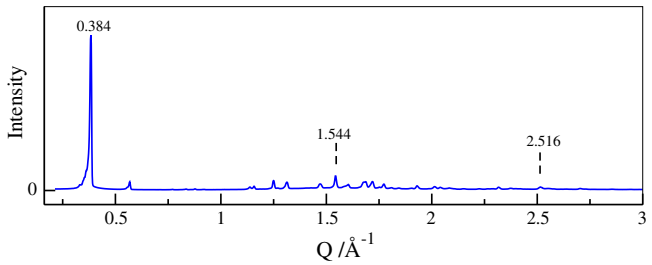

Fig. 4. Cu-Kα Powder diffraction pattern for solid PeAN. The three main features described by Greaves et al. correspond to the peaks highlighted by the dashed lines.

the simulation, we were able to extract some crucial structural information from the trajectory. The simplest geometric information that can be derived is the radial distribution functions (RDF).

Two set of different radial distribution functions are represented in Fig. 5: in the left panel the correlation between the nitrogen atom of the NH_3^+ group and oxygen atoms of the nitrate, and between the Centers of Mass (COMs) of the alkyl chains are shown, while the right panel focuses on the RDFs between the ammonium hydrogen atoms and oxygen/nitrogen of the anion. The simulation highlights a tight first coordination shell centered at about 2.8 Å (heavy atoms), value compliant with other works on similar compounds [15,42,43]. Clearly, the amino group and the anion form a strong hydrogen bond: the relative first peak is very intense. The satellite small peak around 4.7 Å is due to the correlation with the oxygen not involved in the H-bond. Regarding the other RDF of left panel (red curve), we can see that the alkyl chains show a weak correlation that gives rise to a broad peak centered at about 5.0–5.5 Å, with sizable peak broadening due to the length of the chain. It is important to notice that the alkyl chains act as a spacer of the polar parts and ultimately lead to the long-range correlations (mainly between anions) that give rise to the pre-peak [41]. In order to provide a quantitative description of the H-bond network we have calculated the following quantities: the number of oxygen atoms coordinated to the nitrogen atom of the cation and

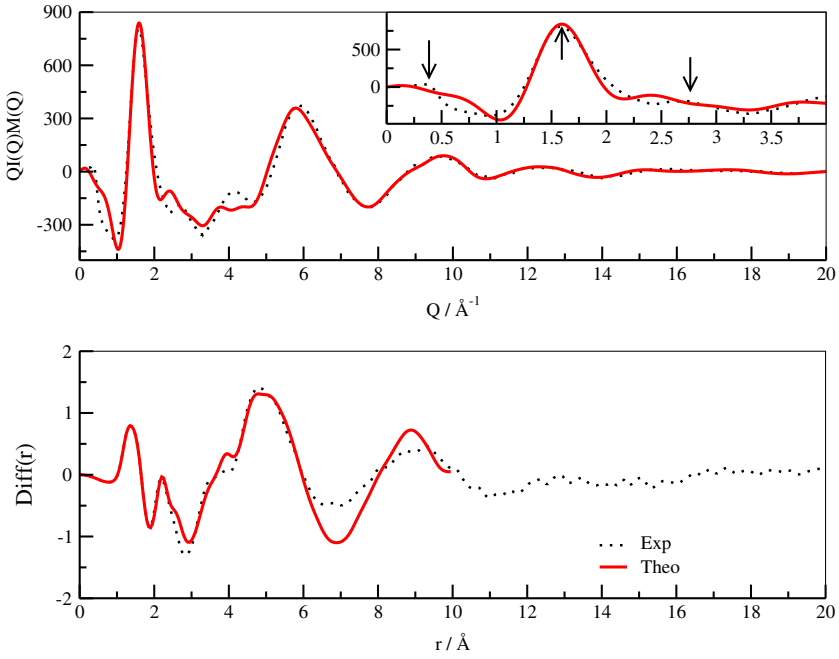

Fig. 3. Theoretical and measured diffraction patterns. Top: Structure function; Bottom: Radial distribution function. The 0–4 $Å^{-1}$ range is reported in the inset; the arrows point to the three peaks described in previous studies at different temperatures by Greaves et al.

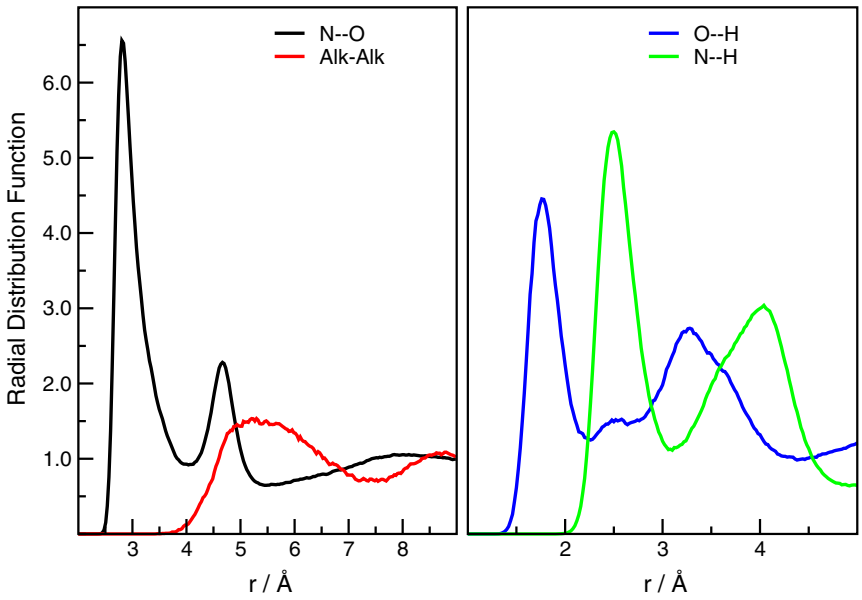

Fig. 5. Left panel: black line: RDF of N··· O distance; red line RDFs between alkyl chains COMs. Right Panel: correlations involving polar hydrogen atoms and anion oxygen (blue) or nitrogen (green)

the average number of H-bond contacts. The former is obtained by integrating the first peak of the relative RDF, while the latter search was performed counting as H-bonds the contacts that satisfied the following distance/angle criteria: N··· O distance included in the range between 0 and 3.5 Å and N—H—O angle between 135 and 180 degrees; the calculation was done with VMD package [44]. We obtained a total of 5.3 oxygen atoms surrounding the cation and an average of 2.6 hydrogen bond contacts. This means that each hydrogen atom of the ammonium group can coordinate more than one oxygen at a time, but not all the oxygen atoms can form H-bonds. Hence, the extracted parameters comply with the results obtained in previous works [14,45], namely that the hydrogen bond network for the anions is not complete, and that roughly just two oxygen atoms of the nitrate are involved in stable hydrogen bonds. In the end, we calculated the H-bond lifetime with TRAVIS autocorrelation function tool [46]. The points were fitted using the function:

$$C(t) = Ae^{(-\frac{t}{\tau 1})} + (1 - A)e^{(-\frac{t}{\tau 2})} \quad (4)$$

where t is the time, A is a normalization constant, $\tau 1$ and $\tau 2$ are the time constants of two dynamic processes. We have chosen this kind of function because two fundamental processes occur in ionic liquids [47]: the first one, faster, is the breaking/formation of a single ion pair, while the second one, slower, is the migration of the such pair outside the net generated by the other ions ("Cage Escape"). The values obtained are 0.16 and 1.55 ps for $\tau 1$ and $\tau 2$ respectively, and are compatible with those found for other ILs belonging to the same family [42,48].

We then calculated the vibrational spectrum of nitrate ion directly from the Fourier transform (FT) of the velocity autocorrelation function, corresponding to the velocity density of states (VDOS). The assignment of each peak was accomplished by projecting the VDOS onto the molecules effective normal modes with the MOLSIM package. The advantage of this method when dealing with condensed phase systems, compared to the standard "static" method normally used for *in vacuo* studies, that consists of geometry optimization plus Hessian matrix diagonalization (in this case of a single configuration containing 32 ion pairs) lies in the direct assessment of temperature and environment effects on the vibrations [14,38].

The final velocity density of states is reported in Fig. 6.

As one can see, the in-plane deformation normal mode (falling at about 705 cm^{-1}), which keeps its double degeneracy, and the ν_2 and ν_1 modes located at about 800 and 1042 cm^{-1} respectively, are only scarcely influenced by the H-bond network and are similar to those of the molecule *in vacuo*. ν_3 suffers a different fate, instead. In principle it would be a doubly degenerate normal mode, characterized by the asymmetric stretching of the N—O bond, but owing to the non-complete saturation of nitrate acceptor groups with H-bonds (see above), the oxygen atoms experience a different environment, and this leads to the loss of degeneracy of the mode.

For this reason, the mode is split into two components (ν_{3a} and ν_{3b}), with a calculated frequency difference of about 84 cm^{-1}. This value is in compliance with the results obtained for other alkylammonium ILs; in particular, this approach was validated and compared with experimental data in [14]. The last analysis performed on PeAN is the potential of mean force (PMF) of the ion pairing. To quantify such interaction, we exploited the

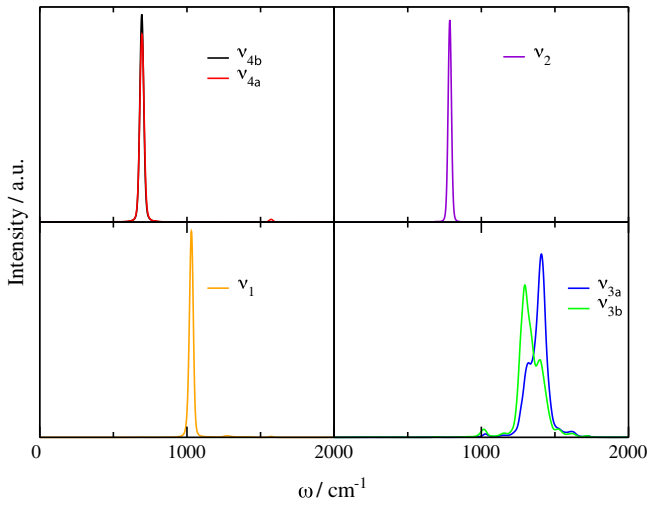

Fig. 6. VDOS of the six normal modes of the nitrate anion. Mode ν_3 (bottom right) experiences a 84 cm^{-1} splitting into ν_{3a} and ν_{3b}

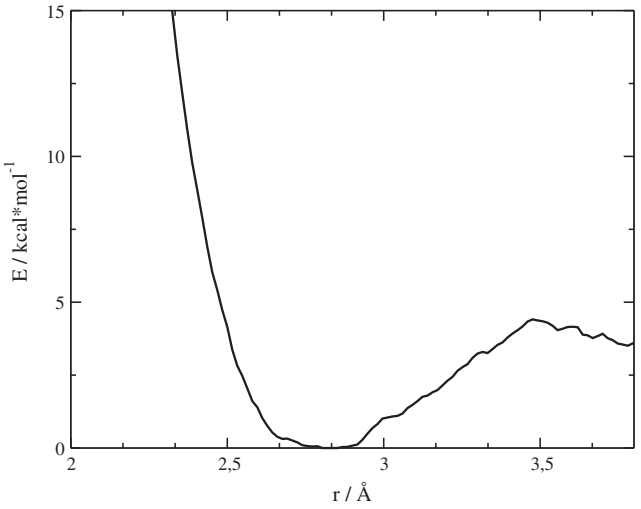

Fig. 7. Cation–Anion Potential of Mean Force *vs* N(cat)···O(ani) distance, calculated with Umbrella Sampling

Umbrella Sampling (U.S.) technique [49], using the N(cat)···O(ani) distance as reaction coordinate. The obtained potential energy profile is reported in Fig. 7.

The cation–anion interaction potential follows a typical Morse-like pattern, whose minimum is located at 2.8 Å, the same value of the maximum position found out in the RDF curve. The magnitude of the interaction is about 4.3 kCal mol^{-1} and it extends up to 3.5 Å, decreasing beyond. The PMF intensity found out for PeAN is similar to the values found for other alkylammonium nitrates [48] but weaker then the values reported for carboxylic acid dimers [50,51] and for another family of ILs, containing choline and aminoacids anions [52].

5. Conclusions

In this work, for the first time, the experimental X-ray scattering profile in the medium-long Q range (0.15–24 $Å^{-1}$) and *ab initio* molecular dynamics simulation for the liquid pentylammonium nitrate are reported. The agreement between experiment and model is very good and enables to trace reliable and relevant structural information about liquid phase. The X-ray pattern agrees with previous published S-WAXS data in the range 0–3 $Å^{-1}$. Our analysis shows that in bulk liquid PeAN, as in many other protic ionic liquids, the cations and anions interact via a hydrogen bond network. The equilibrium N(cat)···O(ani) distance found is 2.8 Å and it is in line with the literature values. The lifetimes of such contacts turn out to be 1.55 ps. Furthermore we find out that even in this IL the nitrate ion exhibits a non-saturated coordination sphere. That is only two of the three oxygen atoms form H-bonds. By the projection of the velocity density of states onto effective normal modes, we have calculated the vibrational spectrum of the anion. The main effect of H-bond interaction on anion vibrations is the loss of degeneracy in the antisymmetric stretching normal modes. The last energetic analysis performed on the ILs shows that the interaction between cation and anion is of about 4.3 kcal mol^{-1}.

Acknowledgements

The authors are deeply grateful to Prof. Ruggero Caminiti (Department of Chemistry, Roma "La Sapienza" University) for his support and for the very helpful discussions and for providing free computing time on NARTEN Cluster HPC Facility. Financial support of the Scientific Committee of the University of Rome through grants C26A13KR5Z, C26A142SCB and C26H13MNEB is also gratefully acknowledged.

References

[1] P. Walden et al., Bull. Acad. Imper. Sci.(St. Petersburg) 8 (1914) 405–422.
[2] K. Seddon, Kinet. Catal. 37 (5) (1995) 693–697.
[3] J.H. Davis, K.J. Forrester, T. Merrigan, Tetrahedron Lett. 39 (49) (1998) 8955–8958.
[4] P. Nockemann, B. Thijs, K. Driesen, C.R. Janssen, K. Van Hecke, L. Van Meervelt, S. Kossmann, B. Kirchner, K. Binnemans, J. Phys. Chem. B 111 (19) (2007) 5254–5263.
[5] M. Petkovic, J.L. Ferguson, H.N. Gunaratne, R. Ferreira, M.C. Leitao, K.R. Seddon, L.P.N. Rebelo, C.S. Pereira, Green Chem. 12 (4) (2010) 643–649.
[6] K.D. Weaver, H.J. Kim, J. Sun, D.R. MacFarlane, G.D. Elliott, Green Chem. 12 (3) (2010) 507–513.
[7] M. Campetella, L. Gontrani, F. Leonelli, L. Bencivenni, R. Caminiti, ChemPhysChem 16 (1) (2015) 197–203.
[8] M. Campetella, L. Gontrani, E. Bodo, F. Ceccacci, F. Marincola, R. Caminiti, J. Chem. Phys. 138 (18) (2013) 184506.
[9] A. Mariani, R. Caminiti, M. Campetella, L. Gontrani, Phys. Chem. Chem. Phys. 18 (4) (2016) 2297–2302.
[10] T.L. Greaves, D.F. Kennedy, S.T. Mudie, C.J. Drummond, J. Phys. Chem. B 114 (31) (2010) 10022–10031.
[11] T.L. Greaves, K. Ha, B.W. Muir, S.C. Howard, A. Weerawardena, N. Kirby, C.J. Drummond, Phys. Chem. Chem. Phys. 17 (2015) 2357–2365.
[12] V. Vchirawongkwin, C. Kritayakornupong, A. Tongraar, B.M. Rode, J. Phys. Chem. B 115 (43) (2011) 12527–12536.
[13] J. Thøgersen, J. Réhault, M. Odelius, T. Ogden, N.K. Jena, S.J.K. Jensen, S.R. Keiding, J. Helbing, J. Phys. Chem. B 117 (12) (2013) 3376–3388.
[14] M. Campetella, D. Bovi, R. Caminiti, L. Guidoni, L. Bencivenni, L. Gontrani, J. Chem. Phys. 145 (2) (2016) 024507.
[15] E. Bodo, A. Sferrazza, R. Caminiti, S. Mangialardo, P. Postorino, J. Chem. Phys. 139 (14) (2013) 144309.
[16] K. Fumino, A. Wulf, R. Ludwig, Phys. Chem. Chem. Phys. 11 (39) (2009) 8790–8794.
[17] S. Zahn, J. Thar, B. Kirchner, J. Chem. Phys. 132 (12) (2010) 124506.
[18] L. Gontrani, R. Caminiti, U. Salma, M. Campetella, Chem. Phys. Lett. 684 (2017) 304–309.
[19] V. Vchirawongkwin, C. Kritayakornupong, A. Tongraar, B.M. Rode, J. Phys. Chem. B 115 (43) (2011) 12527–12536.
[20] L. Tanzi, F. Ramondo, R. Caminiti, M. Campetella, A. Di Luca, L. Gontrani, J. Chem. Phys. 143 (11) (2015) 114506.
[21] G. Prampolini, M. Campetella, N. De Mitri, P.R. Livotto, I. Cacelli, J. Chem. Theory Comput. 12 (11) (2016) 5525–5540.
[22] R. Caminiti, V.R. Albertini, Int. Rev. Phys. Chem. 18 (2) (1999) 263–299.
[23] R. Caminiti, L. Gontrani (Eds.), The Structure of Ionic Liquids, Springer, 2014.
[24] R. Caminiti, M. Carbone, G. Mancini, C. Sadun, J. Mater. Chem. 7 (8) (1997) 1331–1337.
[25] L. Gontrani, F. Ramondo, G. Caracciolo, R. Caminiti, J. Mol. Liq. 139 (1-3) (2008) 23–28.
[26] A.O. Dohn, E. Biasin, K. Haldrup, M.M. Nielsen, N.E. Henriksen, K.B. Mller, J. Phys. B: At. Mol. Phys. 48 (24) (2015) 244010.
[27] R. Salomon-Ferrer, D.A. Case, R.C. Walker, WIREs Comput. Mol. Sci. 3 (2) (2013) 198–210.
[28] J. Wang, R.M. Wolf, J.W. Caldwell, P.A. Kollman, D.A. Case, J. Comput. Chem. 25 (9) (2004) 1157–1174.
[29] J. Hutter, M. Iannuzzi, F. Schiffmann, J. VandeVondele, WIREs Comput. Mol. Sci. 4 (1) (2014) 15–25.
[30] J. VandeVondele, M. Krack, F. Mohamed, M. Parrinello, T. Chassaing, J. Hutter, Comput. Phys. Commun. 167 (2) (2005) 103–128.
[31] J. VandeVondele, J. Hutter, J. Chem. Phys. 118 (10) (2003) 4365–4369.
[32] J.P. Perdew, K. Burke, M. Ernzerhof, Phys. Rev. Lett. 77 (18) (1996) 3865.
[33] S. Grimme, J. Comput. Chem. 27 (15) (2006) 1787–1799.
[34] J. VandeVondele, J. Hutter, J. Chem. Phys. 127 (11) (2007) 114105.
[35] C. Hartwigsen, S. Gœdecker, J. Hutter, Phys. Rev. B 58 (7) (1998) 3641.
[36] S. Nosé, Mol. Phys. 52 (2) (1984) 255–268.
[37] G. Torrie, J. Valleau, J. Comput. Phys. 23 (2) (1977) 187–199.
[38] D. Bovi, A. Mezzetti, R. Vuilleumier, M.-P. Gaigeot, B. Chazallon, R. Spezia, L. Guidoni, Phys. Chem. Chem. Phys. 13 (47) (2011) 20954–20964.
[39] M. Campetella, D. Martino, E. Scarpellini, L. Gontrani, Chem. Phys. Lett. 660 (2016) 99–101.
[40] L. Gontrani, E. Bodo, A. Triolo, F. Leonelli, P. D'Angelo, V. Migliorati, R. Caminiti, J. Phys. Chem. B 116 (43) (2012) 13024–13032.
[41] J.C. Araque, J.J. Hettige, C.J. Margulis, J. Phys. Chem. B 119 (40) (2015) 12727–12740.
[42] E. Bodo, A. Sferrazza, R. Caminiti, S. Mangialardo, P. Postorino, J. Chem. Phys. 139 (14) (2013) 144309.
[43] M. Campetella, M. Montagna, L. Gontrani, E. Scarpellini, E. Bodo, Phys. Chem. Chem. Phys. 19 (2017) 11869–11880.
[44] W. Humphrey, A. Dalke, K. Schulten, J. Mol. Graphics 14 (1) (1996) 33–38.
[45] S. Zahn, J. Thar, B. Kirchner, J. Chem. Phys. 132 (12) (2010) 124506.
[46] M. Brehm, B. Kirchner, J. Chem. Inf. Model. 51 (8) (2011) 2007–2023.
[47] M.G. Del Pópolo, G.A. Voth, J. Phys. Chem. B 108 (5) (2004) 1744–1752.

[48] M. Campetella, M. Macchiagodena, L. Gontrani, B. Kirchner, Mol. Phys. 115 (13) (2017) 1582–1589.
[49] G.M. Torrie, J.P. Valleau, J. Comput. Phys. 23 (2) (1977) 187–199.
[50] T. Neuheuser, B.A. Hess, C. Reutel, E. Weber, J. Phys. Chem. 98 (26) (1994) 6459–6467.
[51] Y. Gu, T. Kar, S. Scheiner, J. Am. Chem. Soc. 121 (40) (1999) 9411–9422.
[52] M. Campetella, S. De Santis, R. Caminiti, P. Ballirano, C. Sadun, L. Tanzi, L. Gontrani, RSC Adv. 5 (63) (2015) 50938–50941.